CENTER FOR RESEARCH AND ADVANCED STUDIES
OF THE NATIONAL POLYTECHNIC INSTITUTE
MONTERREY UNIT

ASSESSMENT OF FETAL BRAIN ACTIVITY SIGNALS IN PREGNANCIES CLASSIFIED AS HIGH RISK

Thesis presented by

Myrthala Wong Tamez

In order to obtain the degree

Master of Science in

Biomedical Engineering and Physics

Advisor: Dr. David Gutiérrez Ruiz

Co-advisor: Dr. Hari Eswaran

Apodaca, Nuevo León, Mexico November, 2017

CENTRO DE INVESTIGACIÓN Y DE ESTUDIOS AVANZADOS
DEL INSTITUTO POLITÉCNICO NACIONAL
UNIDAD MONTERREY

EVALUACIÓN DE LA ACTIVIDAD CEREBRAL FETAL EN EMBARAZOS CLASIFICADOS DE ALTO RIESGO

Tesis que presenta

Myrthala Wong Tamez

Para obtener el grado de

Maestra en Ciencias en

Ingeniería y Física Biomédicas

Director de tesis: Dr. David Gutiérrez Ruiz

Co-director: Dr. Hari Eswaran

Apodaca, Nuevo León Noviembre, 2017

Acknowledgements

Praise God for my life, exactly as it is.

Mother, Diana, and Benito, thanks for your support.

Dr. Dania thanks for your reliance and letting me be part of your research group.

Dr. Hari and Dr. Diana, thanks for your support and guidance at UAMS.

CINVESTAV, thanks for the opportunity, the economic support for my international internship, and for my new friends; thanks Don Nabor for taking care of my papaya plants since I went to Little Rock and to date.

CONACYT, thanks for the economic support and the mixed scholarship.

Félix: I love you. Thanks for your love, care, and unconditional support.

Index

List of figures

List of tables

Abbreviations

BD – Burst duration

bpm – Beats-per-minute

CDC – Centers for Disease Control and Prevention

Cinvestav – Center for Research and Advanced Studies

CNS - Central nervous system

ENDS – Electronic Nicotine delivery systems

fMCG – Fetal magnetocardiography

fMEG – Fetal magnetoencephalography

GA – Gestational age

IBI – Interburst interval

IUGR – Intrauterine growth restriction

MCG – Magnetocardiography

MEG – Magnetoencephalography

mMCG – Maternal magnetocardiography

PSD – Power spectrum density

SARA – SQUID Array for Reproductive Assessment

SNR – Signal-to-noise ratio

SQUID – Superconducting Quantum Interference Device

UAMS – University of Arkansas for Medical Sciences

Abstract

The maturational process of the fetal brain over gestation can be assessed through changes in fetal behavior patterns, both spontaneous and evoked. Hence, in this work we are interested in finding out if there exists a difference between the maturational process of a fetus in a low-risk pregnancy and in a high-risk pregnancy due to smoking, either tobacco or from an electronic nicotine delivery system (ENDS). We recorded the fetal spontaneous brain activity using fetal magnetoencephalography (fMEG) and compared the burst and interburst interval (IBI) duration of seven fetuses (three from smoker mothers and four from non-smokers) during gestational ages (GAs) ranging from 32 to 35 weeks. We found that for both the smokers and non-smokers groups, the IBI mean duration shortens while the GA increases. Furthermore, the mean burst duration for the smokers group was statistically the same, while in the non-smokers group the mean burst duration increased with GA, as physiologically expected. Our preliminary results show that the spontaneous brain activity of a fetus in a nicotine-caused high-risk pregnancy tends to have larger IBIs and smaller bursts. Therefore, our results suggest that the spontaneous brain activity of the fetus is diminished if the mother smokes.

Resumen

El proceso de maduración del cerebro fetal a lo largo de la gestación se puede evaluar a través de cambios en patrones de comportamiento fetal, tanto espontáneos como evocados. Entonces, nuestro objetivo es saber si existe alguna diferencia en el proceso de maduración de un feto en un embarazo de bajo riesgo y uno considerado de alto riesgo debido a que la madre fuma, ya sea cigarrillo normal o electrónico. Obtuvimos la actividad cerebral espontánea fetal usando magnetoencefalografía fetal (fMEG) y comparamos tanto las detonaciones de actividad cerebral como los intervalos entre detonaciones (IBI, por sus siglas en inglés) de siete fetos (tres de madres fumadoras y cuatro de madres no fumadoras) entre las semanas gestacionales 32 y 35. Encontramos que para ambos grupos, fumadores y no fumadores, la duración media de IBI se acorta conforme la edad gestacional progresa. Además, para el grupo fumadores, la duración media de las detonaciones es estadísticamente igual, mientras que para el grupo no fumadores, la duración media de las detonaciones se incrementó con la edad gestacional, tal como se espera fisiológicamente. Nuestros resultados sugieren que la actividad cerebral espontánea del feto en un embarazo de alto riesgo por nicotina tiene IBIs más grandes y detonaciones más cortas. Esto de cierta manera revelaría que la actividad cerebral espontánea del feto disminuye si la madre fuma.

Chapter 1

1 Introduction

The human brain is a complex organ which develops and adapts continuously over lifetime. Despite the noteworthy advances in the area of functional brain research, our understanding of brain processes remains limited (Preissl & Lowery, 2004). Neurophysiological research is mainly focused in brain development from birth to adulthood, but in the last two decades neurophysiological research concerning prenatal human brain development has grown (Muennsinger, Eswaran, & Preissl, 2014).

Recently, it has become possible to assess the maturational process of the fetal brain over gestation by changes in fetal behavior patterns, both spontaneous and evoked (Eswaran, et al., 2012). Prenatal brain studies are significant since detection of risk conditions in an early stage of compromise allows physicians to initiate treatments in order to prevent brain damage. High risk factors in pregnancy include the mother's age, psychological mood, heart diseases, preeclampsia, drug abuse, and smoking, among others.

Research shows that the development of fetuses with high-risk maternal conditions and intrauterine growth restriction (IUGR) appears to be different than in low-risk fetuses (Eswaran, et al., 2012). It is known that tobacco smoking during pregnancy adversely affects intrauterine life, leading to negative effects on the overall fetal

development (Cartney, Fried, & Watkinson, 1994; Hellstrom-Lindahl & Nordberg, 2002; Oliff & Gallardo, 1999). Regarding fetal development, previous studies have related smoking during pregnancy with IUGR, hypoxia, congenital malformations, upregulation of nicotinic acetylcholine receptors, and alteration of excitatory postsynaptic potentials, among others. It has been reported that children and adults who were exposed to nicotine before birth have greater irritability and hypertonicity, emotional and behavioral problems, less focused attention and auditory responses, lower language comprehension, lower IQ, greater reductions in cortical gray matter, and even possible mental retardation (Chi-Yuan, Yu-Jung, Jia-Fu, Chao-Lin, & Chia-Hsiang, 2012). There have been few studies that have examined the effects of smoking on fetal brain over gestation, but their focus has been on brain volume, not in brain activity (Ekblad, et al., 2015).

1.1 Problem

Although post-natal studies have been performed to investigate the harmful effects of tobacco, there are no studies examining the *functional* aspects of the fetal brain in utero that are affected by the mother's exposure to tobacco.

According to Centers for Disease Control and Prevention (CDC) Office on Smoking and Health, the use of electronic nicotine delivery systems (ENDS), including e-cigarettes, has increased rapidly since

their introduction to the US market in 2007. ENDS are often considered by users and some researchers to be safer than conventional cigarettes, even in the case of pregnancy (Regan, Promoff, Dube, & Arrazola, 2013; CDC, 2016).

Our belief is that nicotine alone is enough to affect fetal brain development, independently of the mode of delivery. In this work we study the brain development of fetuses of pregnant mothers who are smokers and/or ENDS users and implement an advanced signal processing technique to enhance the assessment of the fetal brain data.

1.2 Hypothesis

The effects on fetal development of nicotine exposure can be assessed through differences in fetal spontaneous brain activity when compared to low risk pregnancies' spontaneous brain activity.

1.3 Objectives

In order to test the hypothesis, this work has the following objectives:

1.3.1 General objective

To gain knowledge about the effects of nicotine as a risk factor on fetal development through measurements of brain activity.

1.3.2 Specific objectives

- To propose a signal processing scheme to accurately separate fetal brain activity from other signals, especially those of cardiac nature.
- To assess and compare bursts of spontaneous brain activity in fetuses of smoking mothers and those of non-smoking mothers.
- To assess and compare the intervals between bursts of spontaneous brain activity in fetuses of smoking mothers and those of non-smoking mothers.

Chapter 2

2. State of the Art

In this chapter we briefly describe the basis behind brain activity, magnetoencephalography, the SARA system, the normal development of a fetus, and smoking during pregnancy.

2.1 Brain activity

The human central nervous system (CNS) is the most complex organ of the human body. Among its functions, it receives and interprets sensory information, controls behaviors, and participates in the logic process, both inductive and deductive. The CNS is composed by billions of neurons and glial cells. Neurons are specialized nerve cells that send and receive signals through electrical or chemical impulses at their synapses. A neuron may receive thousands of synapses, and acts as an information-processing device (Fundamentals of the Nervous System, 2017).

2.2 Magnetoencephalography

The thousands of electrical impulses generated by brain activity generate electrical currents, and the magnetic field corresponding to those currents can be detected through the scalp (Sheridan, Matuz, Draganova, Eswaran, & Preissl, 2010).

For more than five decades, magnetism has been used to identify neuronal electric activity, being Cohen in 1968 the first one to register the brain activity signal, (Maestú, Gómez-Utrero, Piñeiro, & Sola, 1999), opening the road for magnetoencephalography.

Magnetoencephalography (MEG) is a technique concerned with the detection and interpretation of magnetic fields produced by the brain, and it is widely-used for the investigation of human brain function in adults. As magnetic signals are not distorted by the different layering of biological tissue, MEG is ideal for fetal brain investigation (Muennsinger, Eswaran, & Preissl, 2014; Vrba & Robinson, 2001). Thus, the only noninvasive method available that can be used to directly investigate the functional development of the fetal brain in utero is fetal magnetoencephalography (fMEG).

Among the advantages of fMEG are: (Eswaran, et al., 2012; Lowery, Govindan, Preissl, Murphy, & Eswaran, 2009; Muennsinger, Eswaran, & Preissl, 2014; Vrba & Robinson, 2001):

- it has a superior temporal resolution;
- magnetic fields can be detected outside the boundary of the skin without making direct contact with the body;
- magnetic fields are not distorted by the different layers of tissue;
- as it is passive and non-invasive, it is safe for both the fetus and the mother, and it enables the evaluation of

spontaneous fetal brain activity and fetal brain reactions to auditory or visual stimulation.

These characteristics make fMEG a reliable tool to track fetal neurological development.

2.3 SARA system

As brain magnetic fields are up to 9 orders of magnitude smaller than the environmental magnetic noise, the only detectors capable of resolving such small fields are superconducting quantum interference devices (SQUIDs) (Vrba & Robinson, 2001). Fundamental information regarding the origin and the types of biomagnetic fields that can be measured using SQUIDs is shown in Figure 1[1].

For the purpose of our work, we are interested in signals measured through a SQUID array for reproductive assessment (SARA). Such system is a biomagnetic sensing system based on the MEG technique built specifically for fetal neurological assessment. The world's first SARA system was installed in the University of Arkansas for Medical Sciences (UAMS), in Little Rock, Arkansas, where it has been in successful operation since 2000 (Lowery, Govindan, Preissl, Murphy, & Eswaran, 2009). It consists of 151 primary superconducting sensors which detect biomagnetic fields generated in the body by

[1] Figure 1 is based on information from https://www.ese.wustl.edu/~nehorai/research/ra/back.html.

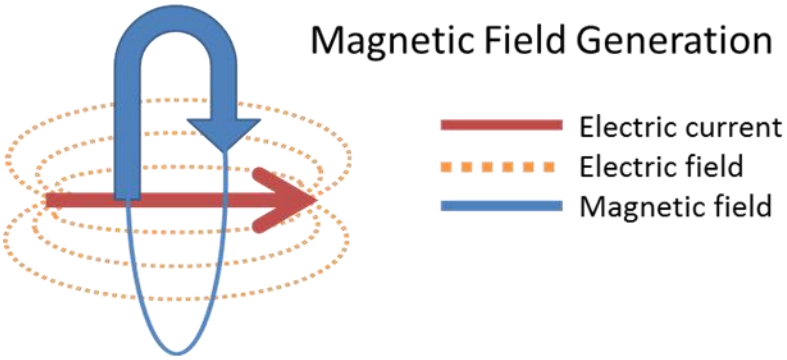

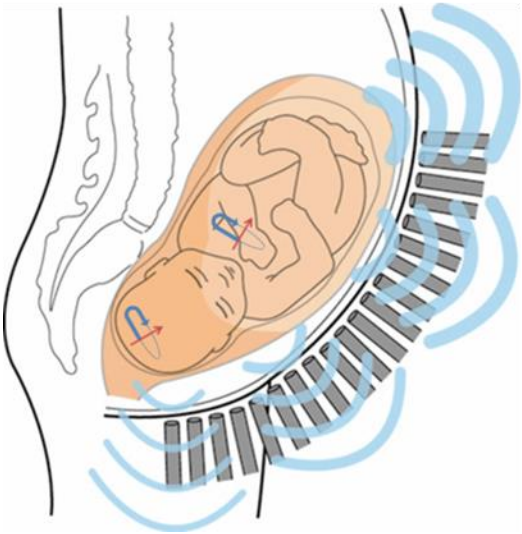

Biomagnetic Field Intensities		
Maternal	**B** (Tesla)	Fetal
Heart (mMCG)	10^{-8}	
	10^{-9}	
	10^{-10}	Heart (fMCG)
Spontaneous brain activity	10^{-11}	
	10^{-12}	Spontaneous brain activity
	10^{-13}	
	10^{-14}	
	10^{-15}	SQUID sensitivity

Figure 1 Biomagnetic Fields. Up: how magnetic fields are generated. Down, left: how magnetic fields leave the body and reach the SARA system's sensors. Down, right: order of magnitude of some biomagnetic fields.

various bioelectric sources such as maternal and fetal heart, fetal brain, and smooth muscles.

The SARA system is completely noninvasive and permits the investigation of fetal and maternal parameters from early gestation until delivery.

When using the SARA system the mother simply sits down and leans forward to the concave array, which was designed to fit the maternal abdomen, as shown in Figure 2.

Figure 2 Left: the SARA system. Right: a pregnant mother seated on the SARA system.

2.4 Normal development

The establishment of a biologic timescale of human development requires observation of a large number of normal individuals of known ages and testing them for measurable items of behavior. Because of individual variations in the development, it is equally important to study the growth and development of a single individual over a prolonged period. If these observations are to be correlated with stages of neuroanatomic development, the clinical and morphologic data must be expressed in comparable units. Early in life, precise age periods are difficult to ascertain because of the difficulty in fixing the time of conception. The average human gestational period is 40 weeks (280 days), but birth may occur with survival as early as about 24 or as late as 49 weeks (a time span of almost 5 months), and the extent of nervous system development

varies accordingly. The chronologic or biologic scale assumes special significance in early prenatal life (Ropper, Samuels, & Klein, 2014).

2.5 Smoking in pregnancy

The effects in the fetus of the mother smoking tobacco or non-tobacco cigarettes are usually seen as an increase in heart rate and a decrease in fetal heart rate (baseline variability) and in fetal movements (Kelly, Mathews, & O'Conor, 1984). Nicotine and carbon monoxide have been identified as two major compounds that may have harmful effects on the developing fetus during pregnancy, as can be hypoxia (Anblaan, et al., 2013). There are other studies that relate smoking during pregnancy with long-term effects known on brain-related characteristics like lower adult intelligence, emotional and behavioral problems, and even mental retardation, as mentioned before.

Chapter 3

3. Methodology

This study was performed in two parts. First, data acquisition and pre-processing were done at the SARA research center of the University of Arkansas for Medical Sciences in accordance with institutional guidelines. Second, data post-processing and statistical analysis were done at the biomedical signal processing laboratory of the Center for Research and Advanced Studies (Cinvestav) of the National Polytechnic Institute, Unit Monterrey.

In the following sections, the methods applied in both parts of the study are explained in detail.

3.1 Data acquisition

A specialized nurse is trained to acquire the data. In the first step, the nurse performs an ultrasound (Voulson 730 expert ultrasound machine manufactured by GE Medical Systems, model AO7269, 2002) to get fetal position, fetal head localization, and additional biometric measurements. She collects this information for all the subjects every time before the fMEG recording. Second, fMEG data is acquired using the SARA system at a sampling rate of 312.5 samples/second and a bandwidth of 0-100 Hz for at least 10 minutes each measurement. Finally, a second ultrasound could be done in case the fetus had moved considerably while the recording was taking place, in order to get the brain's new localization.

Each mother participating in the study is expected to have at least four prenatal examinations starting at week 28 of GA. Generally, each examination is performed every two weeks until week 40 or until labor. For this work, we selected only one pregnant mother per GA per group, to whom we will refer to hereinafter as "subject". The subject selected for one GA may or may not be the same as the one selected for the consecutive GA, and data from the same subject can be found several times in the same group.

3.2 Signal pre-processing for spontaneous brain activity

As the SARA system acquires different biomagnetic signals passively emanating from the maternal abdomen, we have to separate the fetal brain signal from all others considered as "background activity" –including breathing and maternal and fetal heart signals-. For that purpose, we use a frequency subtraction method, which is implemented through spatial filtering techniques. Once this is done, we proceed to identify "clean" windows (segments of time believed to contain only fetal brain activity) by recognizing and discarding the windows in which the brain signal still has cardiac residue by using a three-criterion approach: power spectrum density, maternal magnetocardiography (mMCG) average, and fetal magnetocardiography (fMCG) average. These clean windows are the ones we use in later analysis. All signal pre-processing was implemented in Matlab.

Next we will explain each of the pre-processing methods previously addressed.

3.2.1 Frequency subtraction

This is a method in which a set of reference channels is selected in order to get from them interference of a specific frequency that will be subtracted independently on each sensor in the SARA system.

Figure 3 displays the 151-sensor array of the SARA system, while Figure 4 shows the sensor distribution of the SARA system with the name and position of each sensor (also referred to as "channel"). From these channels we select one that is nearest to the center of the fetal head according to the fetal head position found with ultrasound. This sensor is called "head coil" and is marked in pink in Figure 4. In this figure we also distinguish channels colored in green, which correspond to the "exclusion area". Such exclusion area is calculated to be in a 10 cm radius around the head coil (inclusive) and is considered to be the region with largest fMEG activity, i.e. the fetal head region. Reference channels are selected from outside the exclusion area (shown in blue in Figure 4), where there is no fMEG activity in comparison with the exclusion area.

As maternal and fetal magnetocardiography (MCG) have a strong signal that propagates to most channels, these signals should be removed from the exclusion area channels. Also, the characteristic pattern of adult MCG signals is well-known a-priori, hence we can find their peaks. The quasi-stationary frequency of those R-peaks is then

Figure 3 The 151-sensor array of the SARA system.

used as reference to detect the corresponding signal and then *subtract* it from the rest. This method also gets rid of breathing artifacts. Further details about this method can be found in (Vrba, et al., 2012) and (Escalona-Vargas, Siegel, Murphy, Lowery, & Eswaran, 2017).

Assuming raw data acquired with the SARA system consists only of maternal MCG, fetal MCG, and fetal MEG, and knowing that frequency subtraction detects and removes MCG signals, the procedure to get fMEG from raw data is:

1) apply a band-pass filter between 0.5 and 25 Hz using a Butterworth filter with zero-phase distortion;

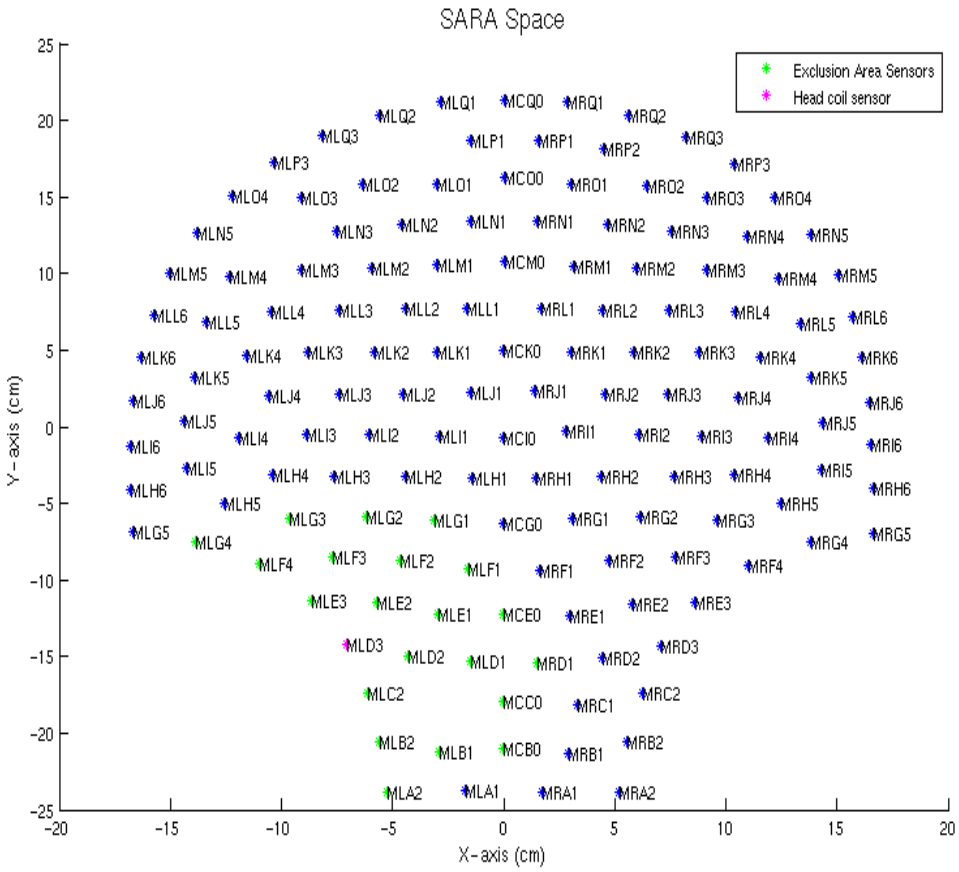

Figure 4 SARA Space showing channel names, exclusion area sensors and head coil sensor.

2) use frequency subtraction to get rid of the maternal MCG signal;

3) use frequency subtraction again, now to get rid of the fetal MCG signal.

As mentioned before, the acquisition period varies for each subject, depending on their comfort and availability. The desirable time length for a spontaneous brain activity study is of 30 minutes, but it could last less. In order to extract fMEG from raw data we divide the signal in windows of one minute duration.

In the subsequent figures, the effect of the frequency subtraction method is shown on three different channels of a non-smoker test subject. The examples correspond to the ninth window, i.e., from minute 8 to minute 9 of the recording, of channels MLF3 and MLF4 of the exclusion area, and channel MRO2 outside the exclusion area.

Figure 5 shows the raw data of the signal once the band-pass filter has been applied. On Figure 6 frequency subtraction has been used to remove mMCG (raw data "minus" mMCG). Figure 7 shows the result of frequency subtraction being used again to remove fMCG (raw data – mMCG – fMCG). According to the stated assumptions, at this point we have fMEG data only. It is important to note that there is no trace of cardiac signals left on channel MRO2, as expected for being outside the exclusion area.

3.2.2 Cardiac residue detection

Once the fMEG signal is isolated from other interfering signals, we want to make sure that the signal left on the exclusion area is fMEG only. Therefore, we developed a method to identify any cardiac residue on our fMEG signal. We evaluated three different criteria: get the power spectrum density of the signal, average the signal at the mMCG R-peaks, and average the signal at the fMCG R-peaks.

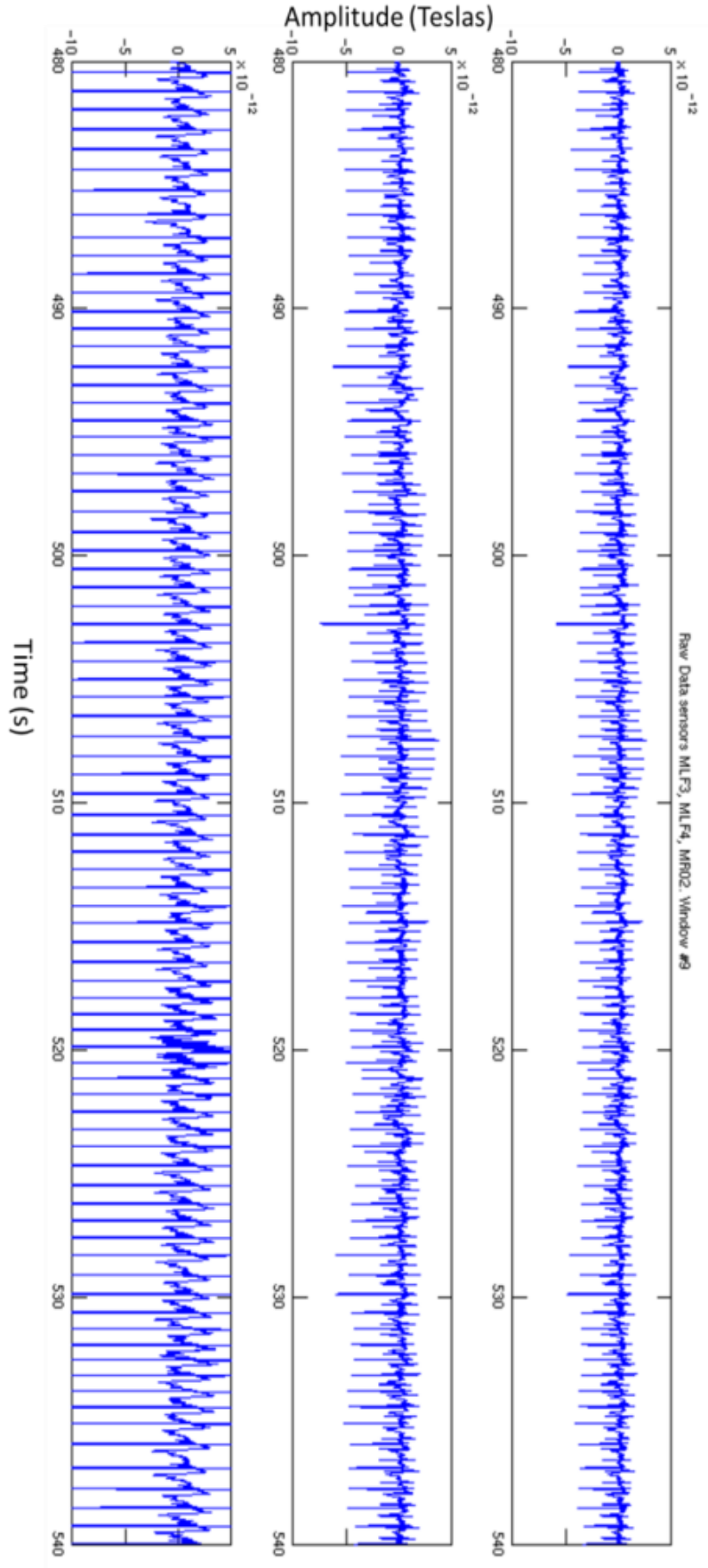

Figure 5 Raw data; window nine, channels MLF3, MLF4, and MRO2.

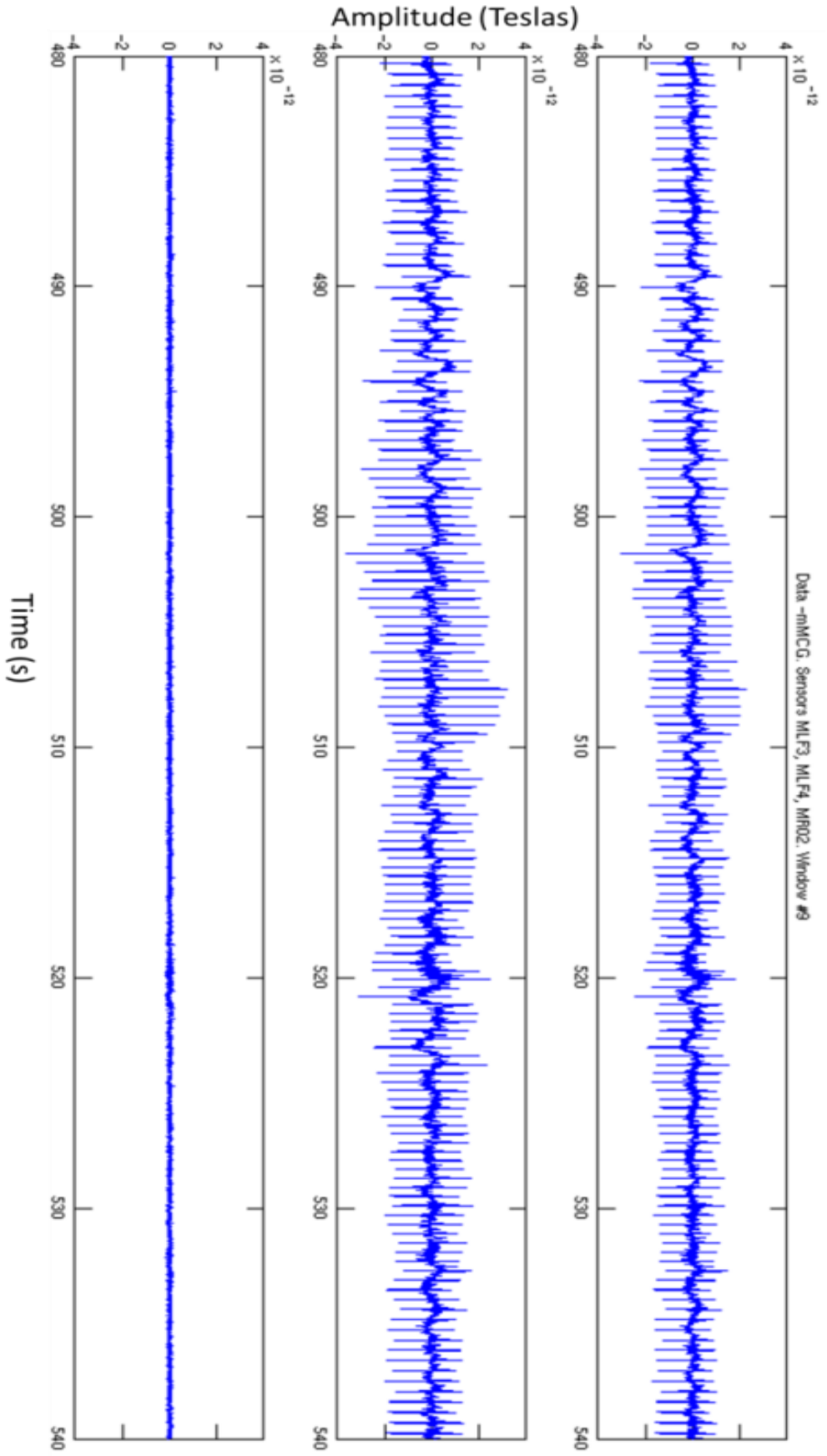

Figure 6 Raw data – mMCG; window nine, channels MLF3, MLF4, and MRO2.

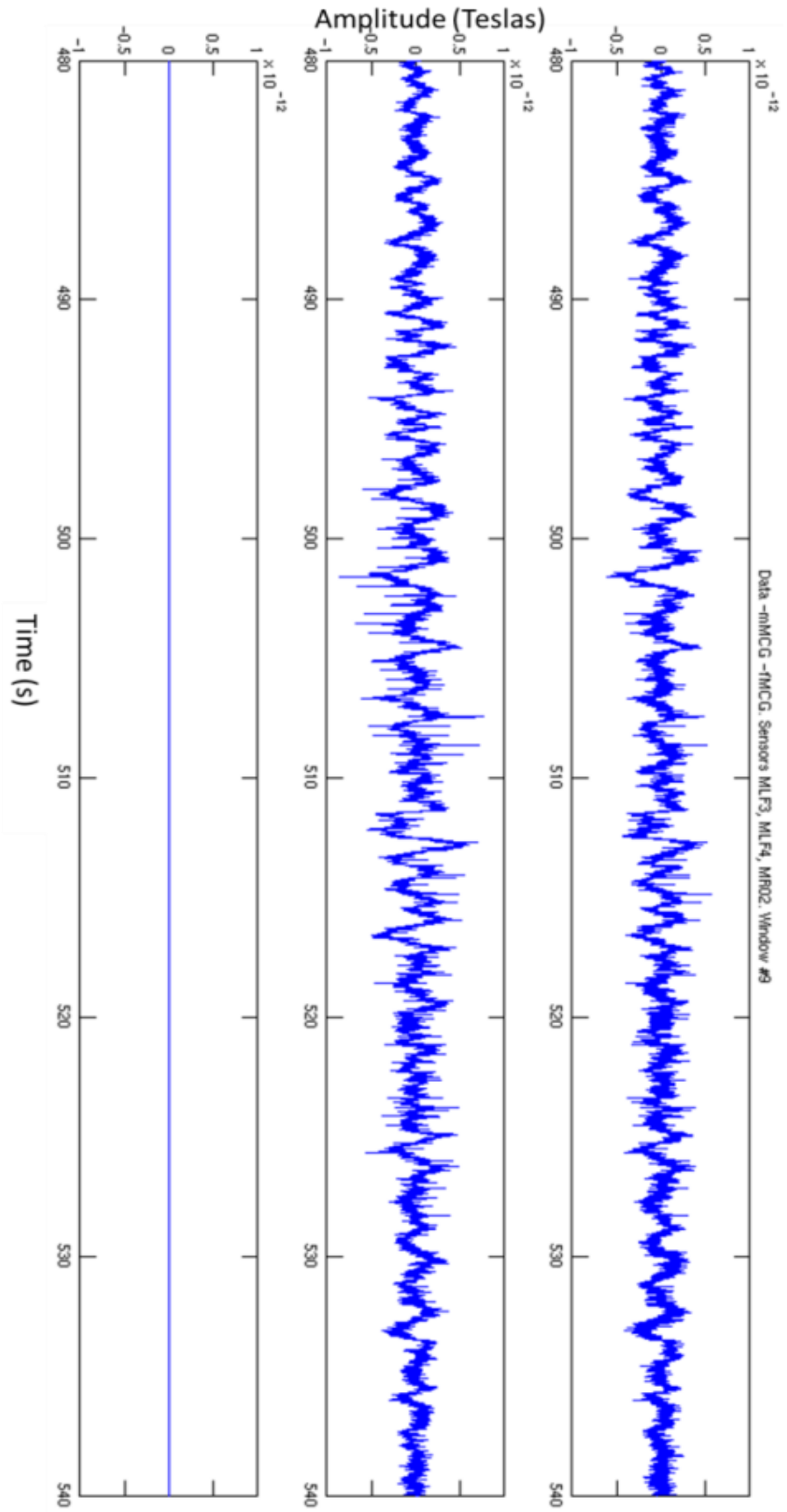

Figure 7 Raw data – mMCG – fMCG; window nine, channels MLF3, MLF4, and MRO2. Notice that on channel MRO2 there is no signal left.

3.2.2.1 Power spectrum density

This stage consists in computing the power spectrum density (PSD) and the signal-to-noise ratio (SNR) of the cardiac signal to differentiate contaminated from clean windows. First, we apply a band-pass filter of 0.5 to 25 Hz to each 60 second window. Then, we select an area of 5 cm around the head coil (inclusive) to compute the PSD of the signal, followed by the calculation of the average power for every window. For example, by considering that fetal heart rate is approximately of 150 beats-per-minute (bpm), and if it is present in the signal, we expect to find peaks at 2.5 Hz or its harmonics.

The SNR we calculate considers the cardiac signal as the desired signal and the fMEG signal as the noise. In order to calculate it, we find the position of a peak, take the average power in it, and divide it by the addition of the average power in that position and the average power in the preceding position. If SNR is greater than 0.59 and in a bandwidth from 0.75 to 15 Hz, the window is considered to be contaminated with cardiac signal, which could be maternal, fetal, or both.

3.2.2.2 mMCG average

In order to make the process of detecting cardiac residue more robust, we added a second criterion, in which we identify if the signal has maternal cardiac residue. Here, we average the fMEG signal at the maternal R-peaks and then we compute the average of its absolute value. If the resulting value is greater than 15 fT (femtoTeslas), that specific window is considered to have mMCG-related contamination.

3.2.2.3 fMCG average

The third and last criterion is used to find fetal cardiac residue. Homologous to the previous stage, first the fMEG signal is averaged at the fetal R-peaks; then, the average of its absolute value is computed. If the resulting value is greater than 10 fT, the window is considered to have fMCG-related contamination.

If a window is considered contaminated by any of the three previously described criteria, that window is discarded from the study in order to work only with clean fMEG signal.

3.3 Signal post-processing for spontaneous brain activity

Once we have the clean windows of the channels near the head coil, we select a *dominant* channel for each subject and measure the burst duration (BD) and the interburst interval (IBI) of the signal.

3.3.1 Interburst intervals and bursts

After clean windows have been identified, we proceed to identify bursts, IBIs, and measure their duration. As a proof-of-concept, here we work only with one channel, to which we refer to as the dominant channel, and now windows are analyzed in two frames of 30 seconds each.

A dominant channel is the most suitable channel for the detection of bursts and IBIs. Its characteristics are:

- it is in the exclusion area;

- ideally, it is located in a 5 cm –radius area around the head coil (inclusive);
- it is one of the least contaminated channels in the exclusion area according to the cardiac residue detection method;
- it is one of the least contaminated channels in the exclusion area according to visual inspection;
- bursts are clearly identified by visual inspection.

SARA research center's crew defined bursts and interburst intervals as follows:

- An interburst interval has a minimum duration of 3 seconds and amplitude ≤50% of the peak to peak amplitude in the burst region.
- A burst doubles the amplitude (>50%) of the IBI region.

As a burst is subjected to greater variability than an IBI, a criterion for its duration was not defined.

Based on the above definitions, computations, and visual inspection, this work defines a burst as a sudden registry of fetal brain activity that starts and finishes at a low peak, whose duration is variable and its amplitude is 50% greater than the IBI's amplitude[2]. When a burst is immediately followed by another burst, or the time

[2] In order to have an objective sense of the amplitude, we took frames with IBI only and calculated the amplitude of peaks. In our data, the samples averaged 40 fT for both smokers and non-smoker subjects.

between bursts is less than 3 seconds, we consider them as a single burst of large duration.

When in a 30-second frame we find both bursts and IBIs, we have a discontinuous pattern. There are two types of discontinuous patterns, defined by SARA research center:

- D1, which corresponds to the presence of at least two bursts interleaved by an IBI in a 30 second window (an example is shown in Figure 8).
- D2, which indicates the presence of a burst with an IBI either at the beginning or at the end of a 30-second window, or the presence of a burst with IBI at both start and end of a 30-second window (see Figure 9).

Continuous patterns are segments which do not adhere to the previously stated definitions of discontinuous patterns, so they qualify for continuous activity. We define a continuous pattern as the presence of bursts throughout a 30-second window or more, as in the example shown in Figure 10.

We plot the windows of the dominant channel in order to find patterns in spontaneous brain activity. From the clean windows plotted we detect burst activity and position a data tip in the start and end of every burst found. In the same time, data tips give us the beginning and end of every IBI. The results of this marking process are recorded in a spreadsheet, where the BD and IBI duration are collected from all the recorded and cleaned data.

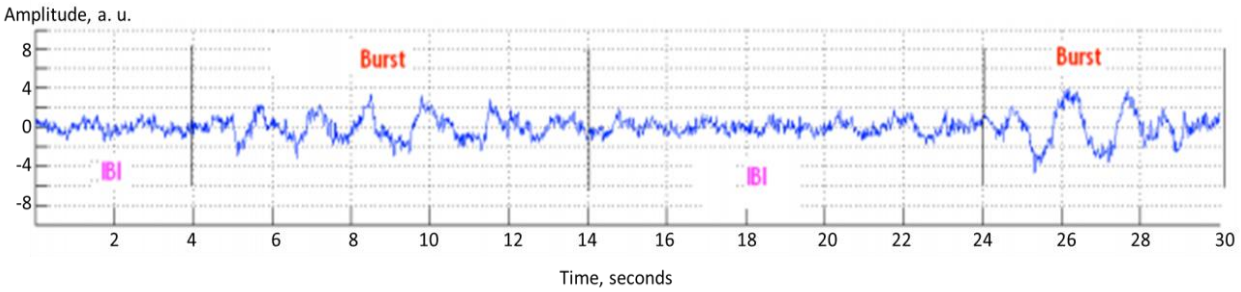

Figure 10 Example of type D1: at least two bursts interleaved by IBI.

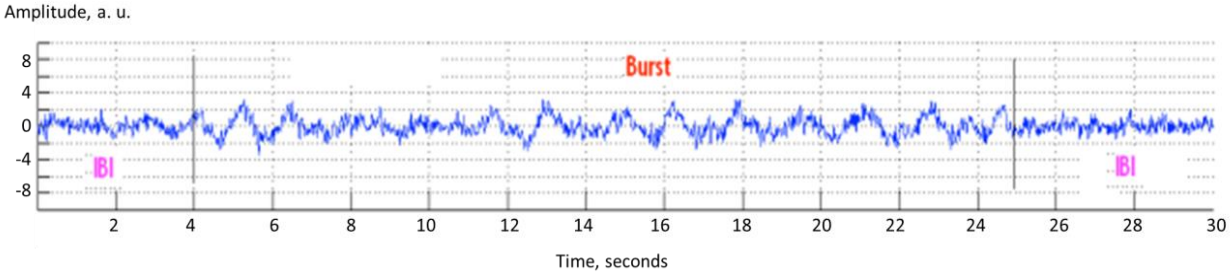

Figure 9 Example of type D2: a burst in presence of IBI, either at the beginning of the window, at the end, or both sides.

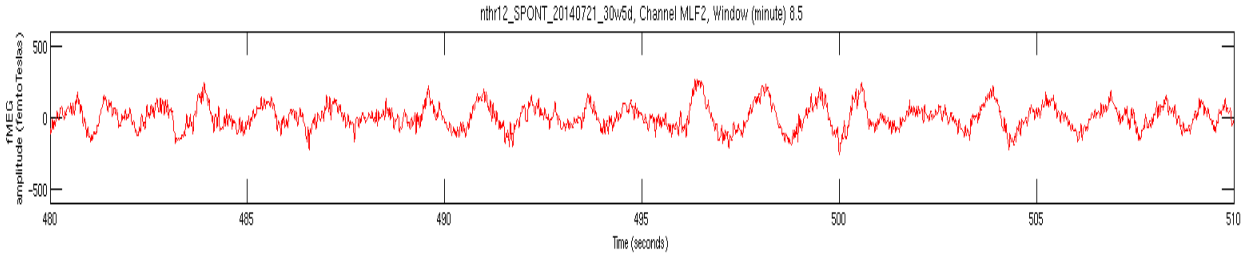

Figure 8 Example of continuous burst pattern present in the dominant channel of a smoker.

3.4 Statistical methods

As the four collected measurements (Smokers IBI, Smokers Burst, Non-smokers IBI, and Non-smokers Burst) have different amount of samples and include nominal and categorical data, we

consider the non-parametric tests of Wilcoxon and Kruskal-Wallis to analyze them.

The Wilcoxon Test is the non-parametric analogue to the paired t-test and it is used to compare two nominal variables and one measurement variable (McDonald J. H., 2014). The test assumes that the two samples are independent and can have different lengths, and it only requires enough data to sort the observations from two sample groups (Haynes, 2013). The first step to this test is to rank the absolute value of the differences between observations from smallest to largest, where the smallest difference ranks 1 and equal differences rank to ties. Then, the ranks of all differences are added in the other direction. The smaller of these two sums is the test statistic. When using this test in Matlab, among the output values we have: the p-value (p) and the result of the hypothesis test (h), respectively. The p-value is a number between 0 and 1, while h is either 0 or 1. The null hypothesis of a Wilcoxon test is that the median difference between pairs of observation is zero. When h=0 it indicates a failure to reject the null hypothesis at a certain significance level, and when h=1 it approves the rejection of the null hypothesis.

The next step is to use Kruskal-Wallis test to compare clusters, which in our study correspond to non-smokers IBIs, non-smokers bursts, smokers IBIs, and smokers bursts. Kruskal-Wallis is the non-parametric analogue to the one-way ANOVA, and it is used when one nominal variable and one measurement variable that does not follow

a normal distribution are compared (McDonald J. H.). In this process, we need to convert the measured observations into their ranks. Similarly as in Wilcoxon test, the smallest observation is ranked 1, the second-smallest is ranked 2, and so on. Tied observations get averaged ranks, too. Also, this test assumes that the different groups have the same distribution. We calculate the sum of the ranks for each group, corresponding to the statistic H, which is approximately chi-squared distributed. The null hypothesis of a Kruskal-Wallis test is that the mean ranks of the groups are the same. After this, a multiple comparison test can be performed to compare each GA's means. The result of the multiple comparison test is a plot of intervals, in which two group means are significantly different if their intervals are disjoint. In the other hand, if the intervals overlap, there are no significant differences between them.

Chapter 4

4. Experiments and results

4.1 Subjects

Even though we are interested in characterizing the spontaneous brain activity of fetuses, our study groups are named after their mothers, specifically under the basis of them being smokers or not and, therefore, if their pregnancy is low-risk or high-risk. In spite of this, we have two groups: *smokers* and *non-smokers*.

4.1.1 Recruited population

The non-smokers group, which corresponds to our control group, is formed by four non-smoking mothers between 29 and 36 weeks of GA, while the smokers group consists of three smoking mothers between 29 and 36 weeks of gestational age (GA), as seen in Table 1. The GA of the fetus was determined by a licensed physician on the corresponding clinical visit, while the smoking status was provided by the mother. Information about the mother's smoking habits is considered confidential for this protocol.

4.1.2 Exclusions

We excluded mothers with pregnancy-related maternal hypertension, chronic hypertension, and/or diabetes. Mothers were also out of the study if their fetus presented a malformation or genetic disease, if the pregnancy was multiple, and if the fetal position was bridge.

Non-smokers	
Subject	**GA**
Prog22	29w6d
Prog02	30w1d
Prog52	31w6d
Prog09	32w0d
prog01	33q1d
Prog22	34w3d
Prog52	35w0d
Prog09	36w0d

Smokers	
Subject	**GA**
nthr12	29w5d
nthr12	30w5d
nthr12	31w5d
nthr12	32w6d
hr209	33w6d
hr211	34w1d
hr211	35w1d
hr211	36w1d

Table 1 Subjects and their corresponding gestational ages.

4.2 Results

We already presented the effect of the frequency subtraction method in the raw signal. Next, we show the work done on the isolated fMEG signal of the exclusion area channels of a non-smoker subject.

As previously explained in the methodology, first we implemented the cardiac residue detection method. For the first criterion, based on the computation of the PSD, we show in Figure 11 the plot of average power vs frequency of the exclusion area channels, in which we identified the peaks and their harmonics at 2.5 Hz. With this information we calculated the SNR of the signal, which tells us if the window is clean or contaminated with cardiac signal. Figure 12 shows the result of this process, where clean windows are shown in blue. As previously defined, if SNR is greater than 0.59 and in a bandwidth from 0.75 to 15 Hz, the window is considered as contaminated with cardiac signal.

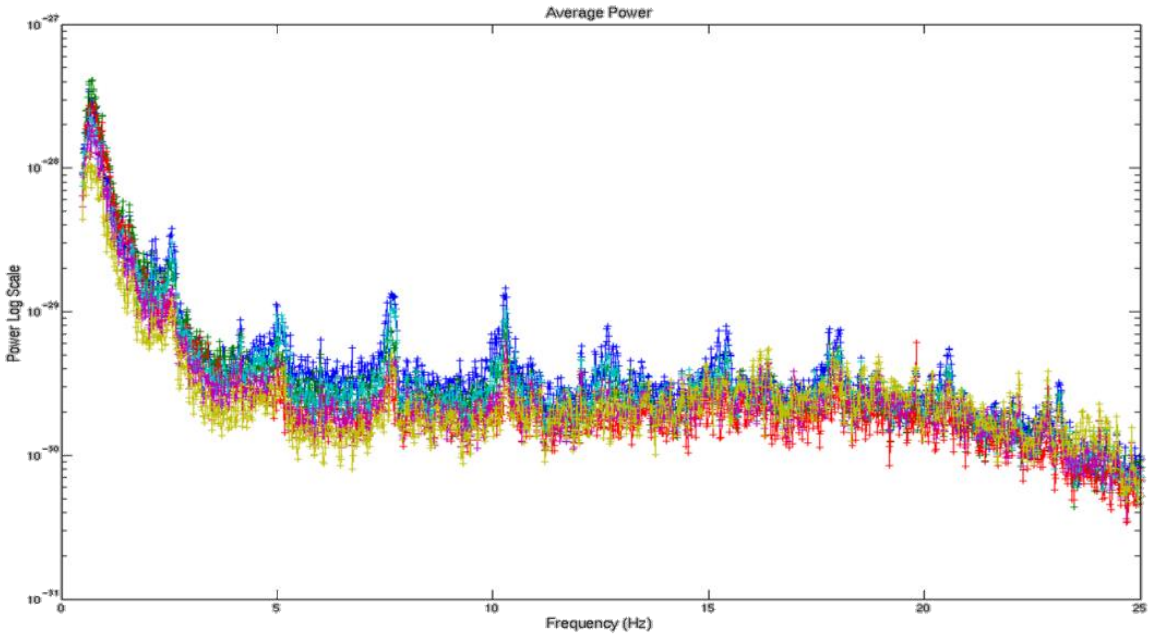

Figure 11 Average power (decibels in log scale vs Hz) of exclusion area channels.

The next two criteria are those in which we identified maternal and fetal cardiac residue on the fMEG signal. Figure 13 shows in blue the windows were the signal has no maternal cardiac residue, while Figure 14 shows in blue the windows where there is no fetal cardiac residue.

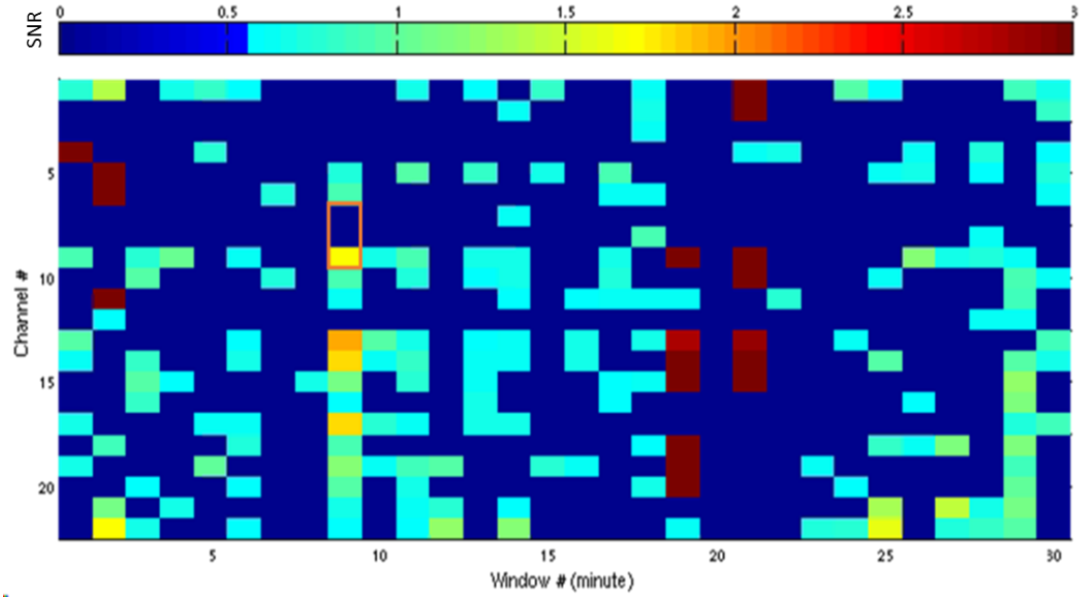

Figure 12 PSD criterion. Clean windows in blue: SNR<0.59 in a 0.75-15 Hz bandwidth.

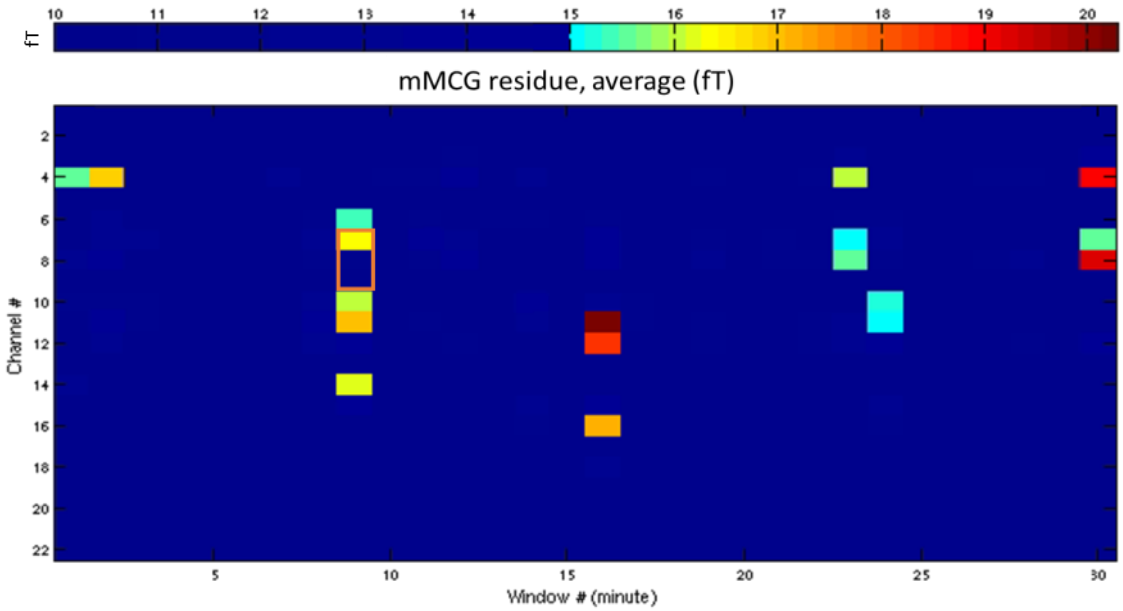

Figure 13 Windows with no mMCG residue in blue.

Figure 15 displays the SARA space, with the exclusion area sensors labeled. In Figures 12, 13, and 14, there are three channels in which the ninth window is selected and shown in an orange rectangle. Those channels are MLF3, MLF4, and MCE0. Figure 15 shows the exclusion area, from which we can locate those three channels. Notice that channels MLF3 and MLF4 are near the head coil and MCE0 is far from the head coil.

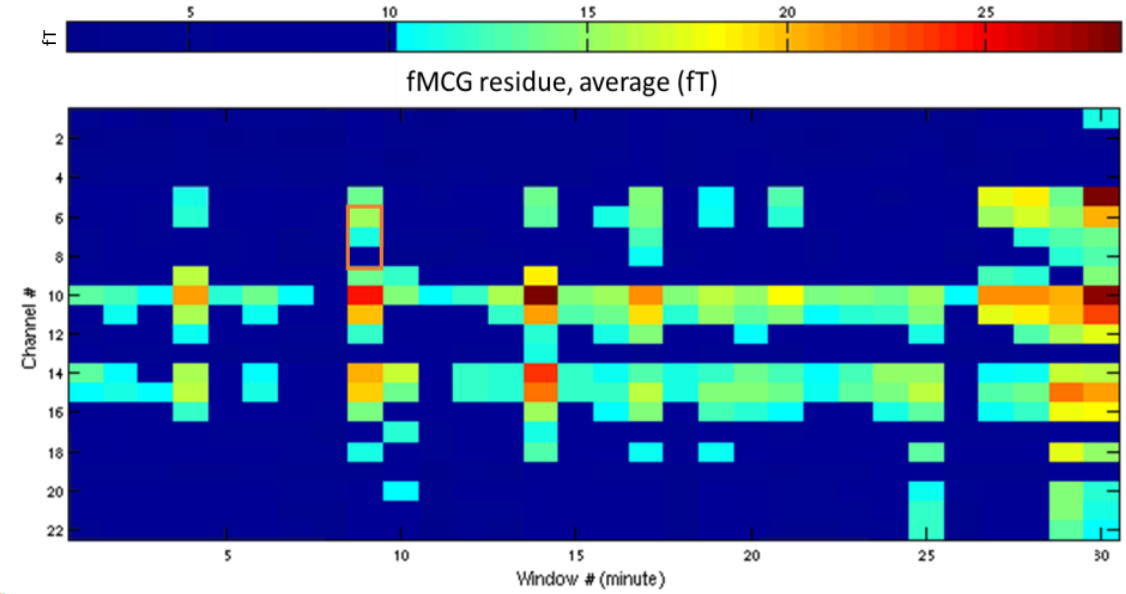

Figure 14 Windows with no fMCG residue in blue.

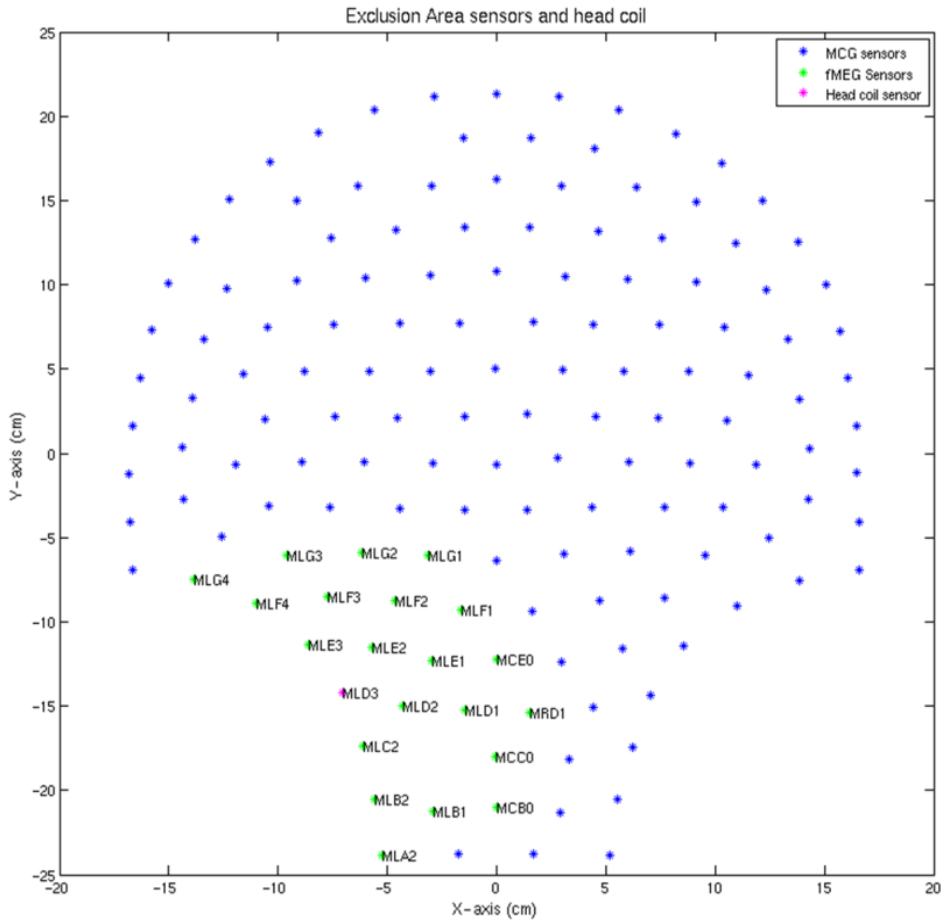

Figure 15 SARA Space showing the exclusion area sensors with labels.

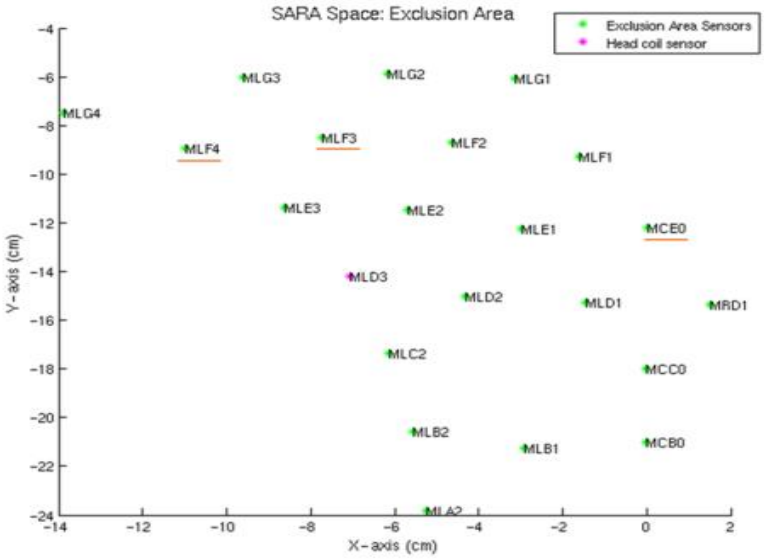

Figure 16 Exclusion area. The underlined channels are the ones selected for the cardiac residue detection process.

Figure 17 shows the signal from the ninth window of the three mentioned channels. Note that channels MLF3 and MLF4 have a clearer fMEG signal than channel MCE0.

After identifying the clean windows, we selected the dominant channel from which we calculated the IBI and burst duration. The results of both IBI and burst duration for every GA of the non-smokers group are shown in Table 2. The column "mean" refers either to the mean duration of the IBIs or of all bursts found in the clean windows of the dominant channel for the corresponding subject. In the same way, the table shows the minimum and maximum duration of IBIs and bursts. It also displays the mean of the means for all GAs, as well as the mean of the minimums and maximums for all the subjects. Finally, the standard deviations for the means, minimum, and maximum values of IBIs and bursts are shown.

Table 3 displays the results of both IBI and burst duration for every GA of the smokers group. The column and row titles and data below the table are homologous to those of the non-smokers group in Table 2.

As stated in the methodology, the measurements (smokers IBI, smokers burst, non-smokers IBI, and non-smokers burst) have different amount of samples and include nominal and categorical data. In addition, we found that they do not follow a normal distribution either, so we compared the groups using the non-parametric tests Wilcoxon and Kruskal-Wallis.

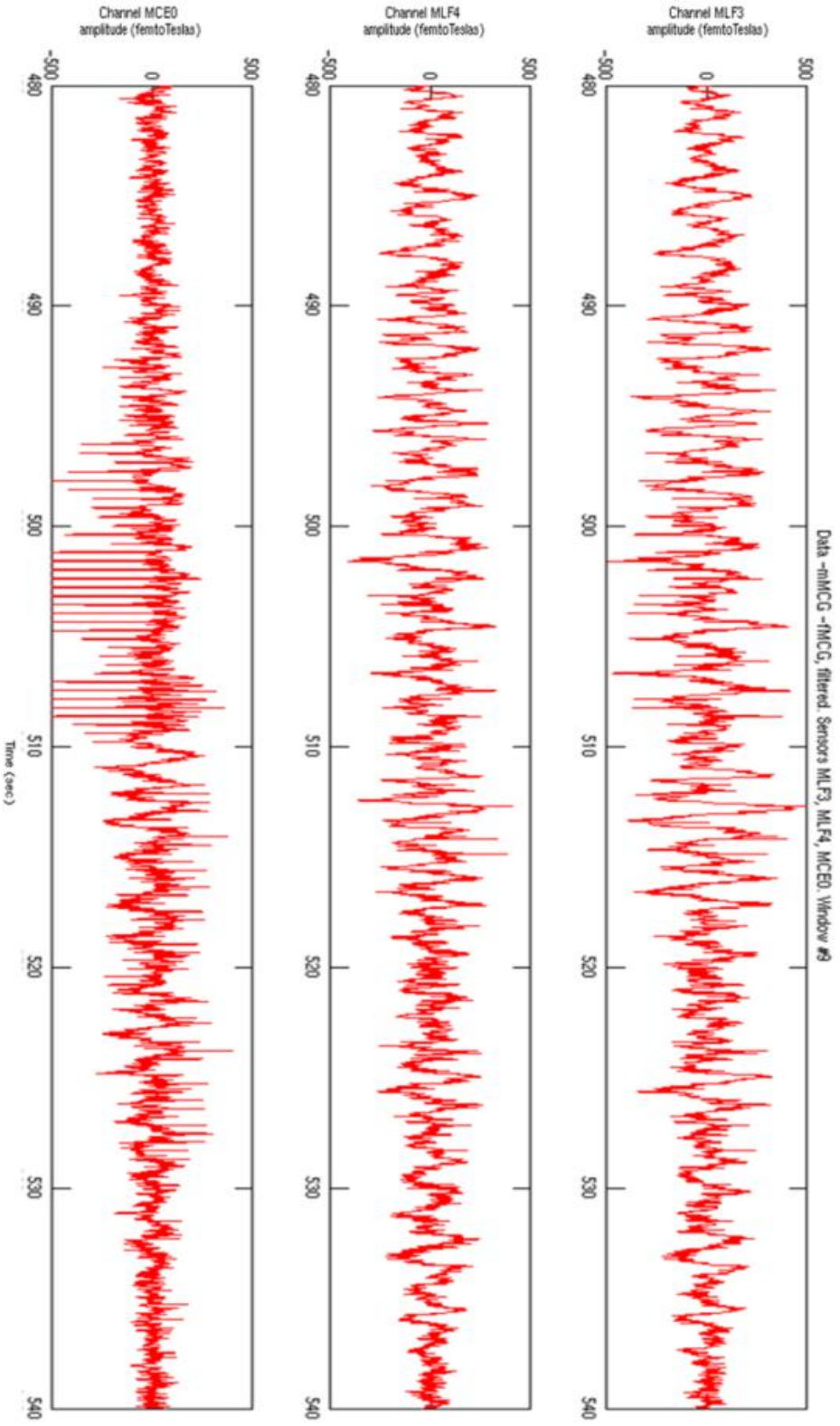

Figure 17 Window 9 of channels MLF3, MLF4, and MCE0 showing filtered fMEG.

Non-smokers						
	IBI duration			Burst duration		
GA	Mean	Min	Max	Mean	B min	B max
29w6d	27.8	3.1	215.7	3.4	0.4	16
30w1d	9.5	3.18	25.62	10.2	0.6	51.5
31w6d	19.2	3	104.8	7.3	0.5	52.2
32w0d	35.4	8.5	180	2.4	0.53	5.8
33w1d	10.4	3.2	36	11.3	0.5	80.4
34w3d	14.1	3	81.1	10.3	0.6	68.5
35w0d	19.8	3.13	85.8	5.8	0.5	31.12
36w0d	12.3	3	118.2	23.5	0.9	137
Mean	18.6	3.8	105.9	9.3	0.6	55.3
Std-dev	9.1	1.9	65.5	6.6	0.1	41.5
Mode	--	3	--	--	0.5	--
		Min IBI	Max IBI		Min burst	Max burst
		3	215.7		0.4	137

Table 3 Non-smokers' mean, minimum, and maximum IBI and burst duration for every GA and other statistics.

Smokers						
	IBI duration			Burst duration		
GA	Mean	Min	Max	Mean	B min	B max
29w5d	62.6	5.4	178.758	6.1	0.4	15.8
30w5d	5.4	4.7	6	57.5	30	85.3
31w5d	54.9	34.6	60	25.4	25.4	25.4
32w6d	5.7	8.5	180	2.4	0.53	5.8
33w6d	13.3	3.8	46.8	8.5	0.5	33.3
34w1d	7.3	3.523	17.3	24.5	0.8	236.7
35w1d	13.5	3.8	35	5.8	0.5	29.6
36w1d	14.7	4.1	30	2.4	0.2	6.4
Mean	22.2	8.6	69.2	16.6	7.3	54.8
Std-dev	23.0	10.6	70.0	18.9	12.7	77.7
Mode	--	3.8	--	--	0.5	--
		Min IBI	Max IBI		Min burst	Max burst
		3.523	180		0.2	236.7

Table 2 Smokers' mean, minimum, and maximum IBI and burst duration for every GA and other statistics.

We used the Wilcoxon test to make a group out of our subjects. The nominal variables were our groups (smokers and non-smokers) and the GAs, while our measurement variable were either the median of the BD or of the IBI. We compared each smokers GA vs the corresponding non-smokers GA at a 95% significance level to find out if they were different. In this case, our null hypothesis was "H0: the median difference between smokers' GA 29 and non-smokers' GA 29 is zero". We performed such testing procedure for each GA.

Table 4 summarizes our results, which show that burst medians of the smoker and the non-smoker groups were the same, except for the fetuses on GA 36. Meanwhile, the IBI medians of GAs 29 and 31 were found to be different. Using this information we decided to consider GA 32 to GA 35 as a single group, corresponding to the last months of pregnancy.

The next step was to use Kruskal-Wallis test to compare four clusters:

Wilcoxon Test				
GA	**Bursts**		**IBI**	
	p	h	p	h
29w	0.8956	0	0.0093	1
30w	0.9975	0	0.8571	0
31w	0.9279	0	0.002	1
32w	0.3171	0	0.2977	0
33w	0.4292	0	0.2037	0
34w	0.8678	0	0.2721	0
35w	0.6589	0	0.6497	0
36w	0.0035	1	0.1133	0

Table 4 Wilcoxon Test comparing the Smokers and Non-Smokers groups by GA. p is the p-value and h refers to the rejection or acceptance of the null hypothesis.

non-smokers IBIs, smokers IBIs, non-smokers bursts, and smokers bursts. The null hypothesis of the Kruskal-Wallis test was, for the non-smokers IBIs: "H0: the mean ranks of the Gas 32 to 35 are the same". We tested this hypothesis on the four clusters and observe their corresponding results in the Kruskal-Wallis whiskers plots below. We also made a multiple comparison test to compare each GA's means as described in the methodology. Figures 18 to 21 show both the Kruskal-Wallis whiskers plots and the multiple comparison intervals.

The whiskers plots display a summary of the set of data: minimum, first quartile, median, third quartile, and maximum. Additionally, they show outliers, if any. If we sort our data from least to greatest, the median is the number in the middle of the list: it has the same amount of values to the left as it has to the right. If data consists of an even amount of numbers, the median is the arithmetic mean of the two middle values. The first quartile is the middle of the first half of numbers, and the third quartile is the middle of the second half of numbers. Finally, a value is considered an outlier when it is less than one and a half times the first quartile or more than one and a half times the third quartile.

Figure 18 shows, on top, the whiskers plot for the IBI duration of the smokers group. Notice that as the GA increases, the IBI duration mean rank decreases. Below the whiskers plot we can see a multiple comparison plot for the same group. Also notice that the mean IBI duration for GAs 32 and 33 are significantly different from GA 35, where the IBI mean duration is shorter.

Similarly, Figure 19 shows, on top, the whiskers plot for the IBI duration of the non-smokers group. Here, even though the IBI duration mean rank is decreasing with GA, their difference is not significant. Again, below the whiskers plot, we show the multiple comparison plot for this group. In this case we observe that the mean duration of the IBI shortens with GA, but again it is not significant.

Likewise, we compared the BD for smokers and non-smokers. Figure 20 shows the whiskers plot of the BD for the smokers, where the mean ranks for all the GAs in the group remain statistically the same. The multiple comparison plot shows that, even when the BD increases from GA 32 to GA35, their mean duration is statistically the same.

In Figure 21 the whiskers plot of the BD for the non-smokers shows a slight increase in the mean ranks for the BD, they are statistically the same. The multiple comparison plot shows how from GA 33 to GA 35 the mean duration of the burst increased. However, as we had continuous patterns in GA 32, the difference among the means for this group is statistically the same.

It is important to notice that for the smokers group, GAs 32 to 35, there are all different subjects, while in the non-smokers group we have information from the same subject for GAs 34 and 35, while for the other two GAs we have different subjects.

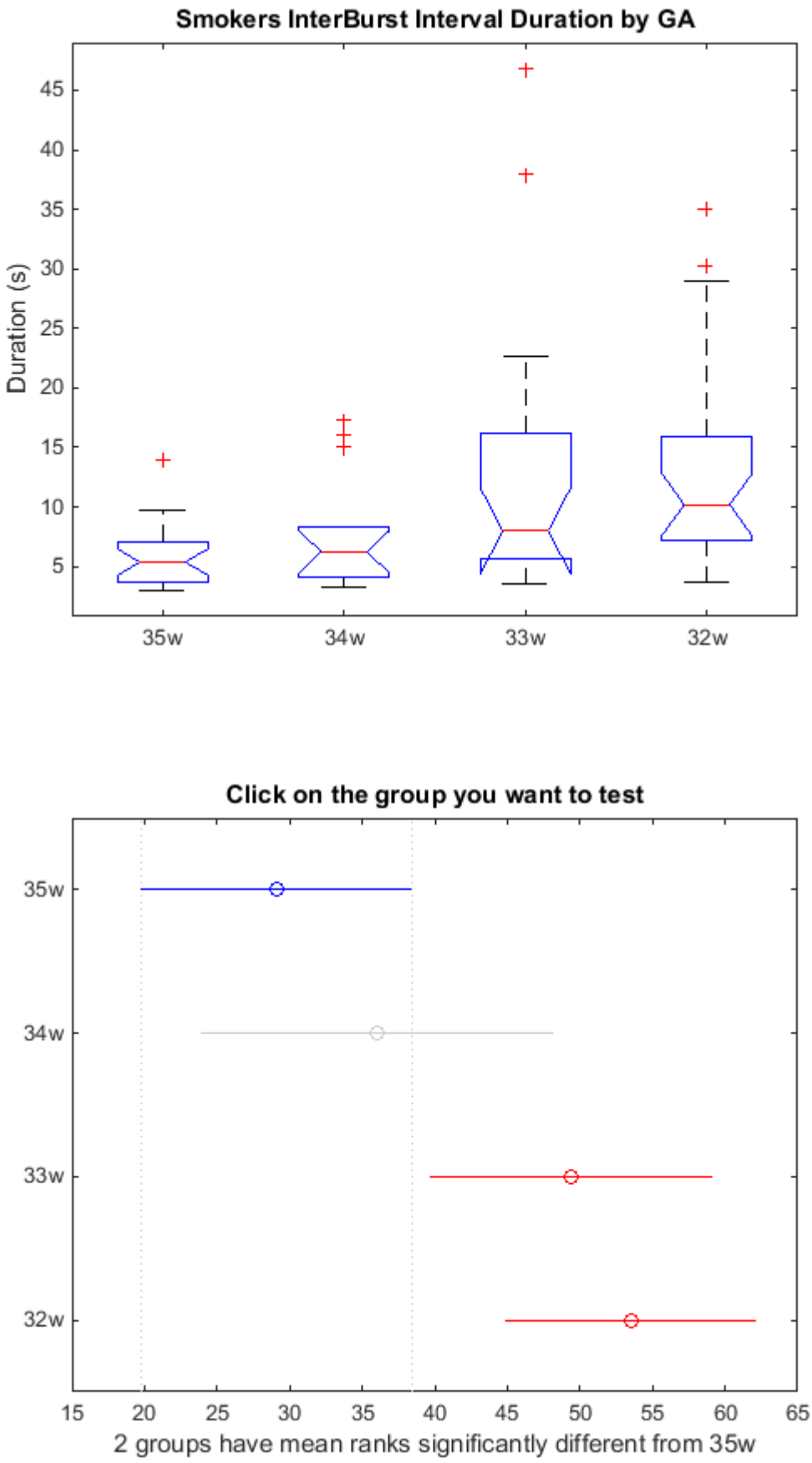

Figure 18 Top: whiskers plot for smokers IBI duration for GAs 32-35. Bottom: the multicomparison graph of each GA's mean IBI duration of the same group.

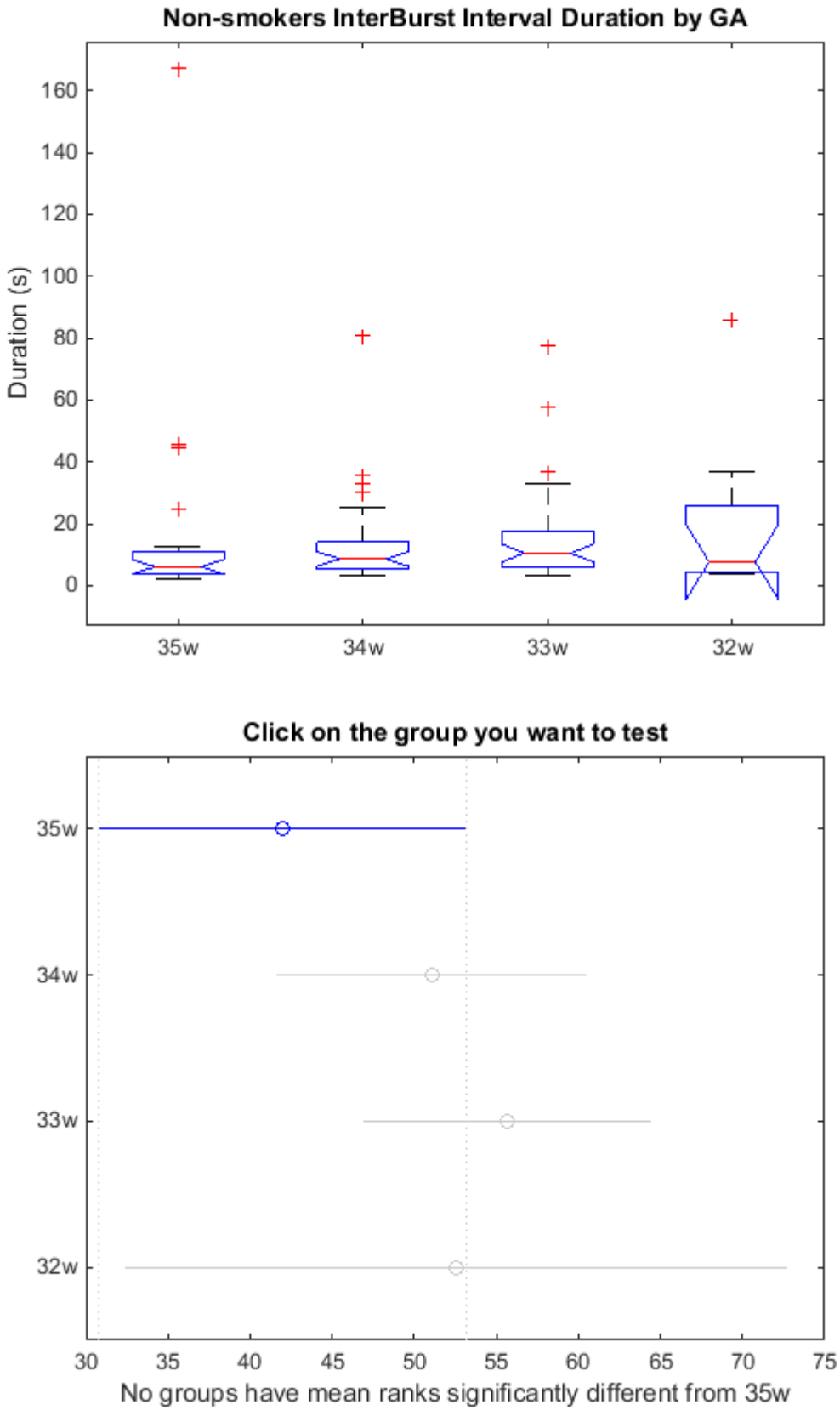

Figure 19 Top: whiskers plot for non-smokers IBI duration for GAs 32-35. Bottom: the multicomparison graph of each GA's mean IBI duration of the same group.

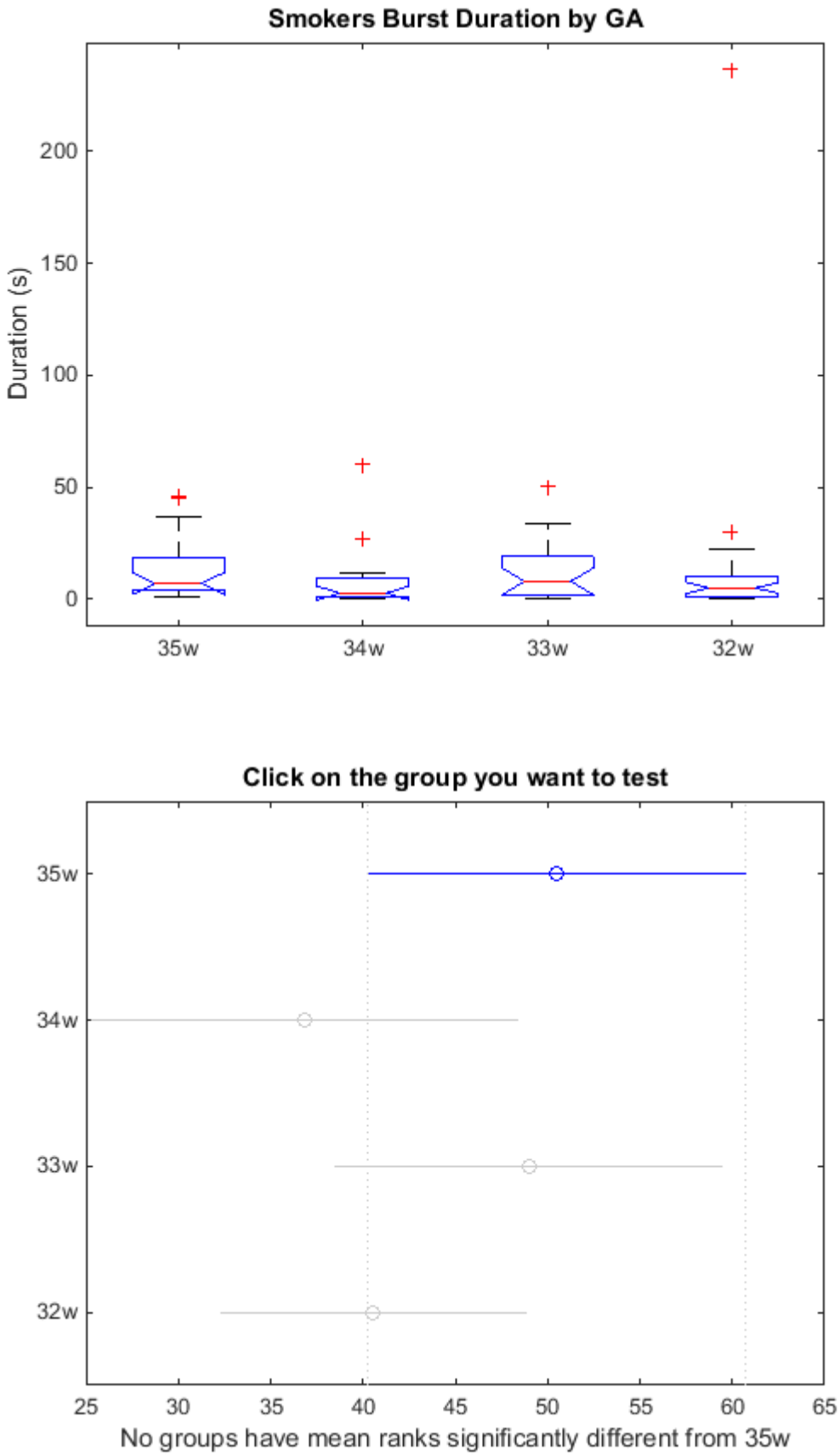

Figure 20 Top: whiskers plot for smokers BD for GAs 32-35. Bottom: the multicomparison graph of each GA's mean BD of the same group.

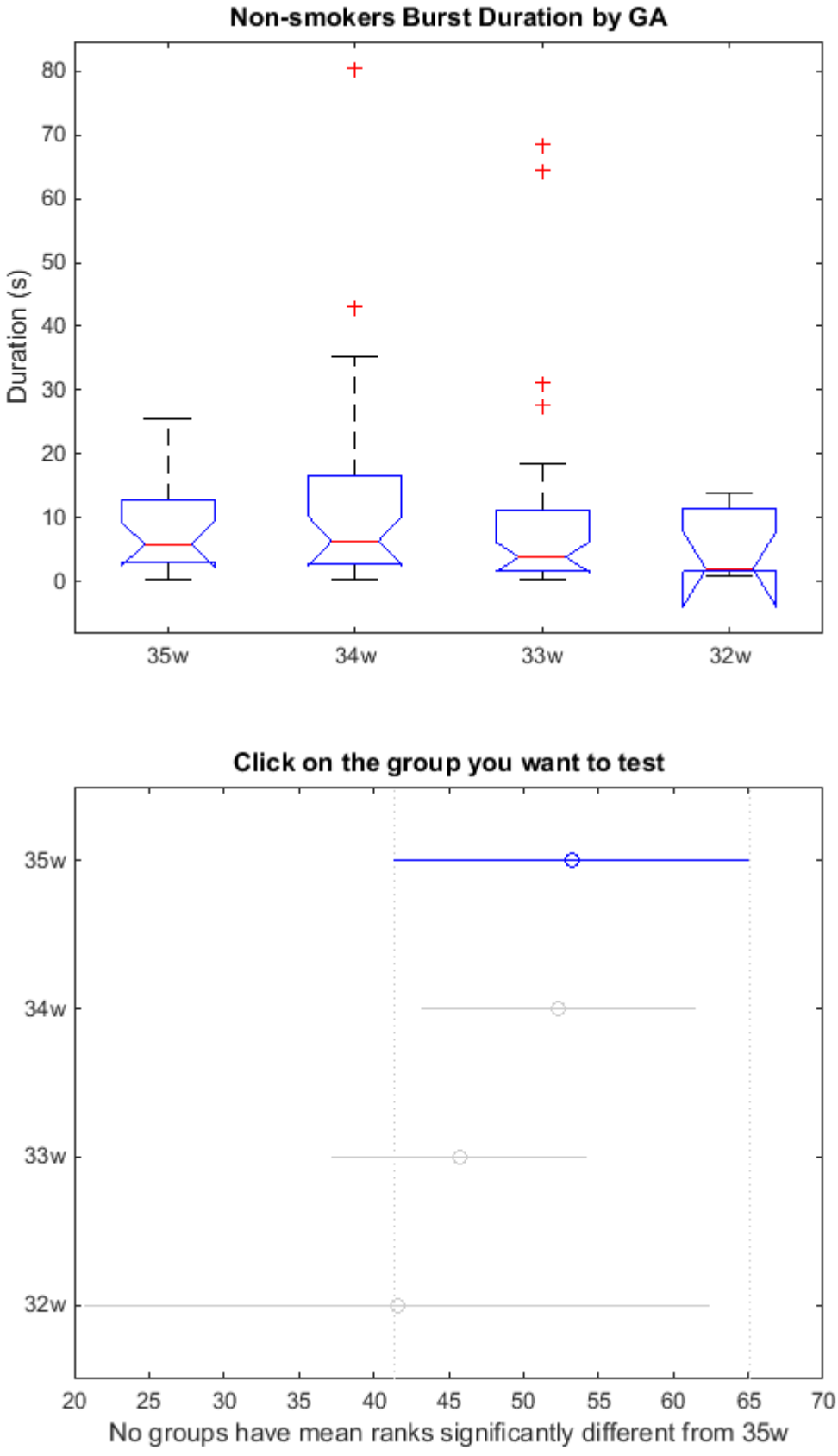

Figure 21 Top: whiskers plot for non-smokers BD for GAs 32-35. Bottom: the multicomparison graph of each GA's mean BD of the same group.

4.3 Discussion

Although medians of every gestational age for both groups are not significantly different, we can observe that the burst duration in the smokers group is shorter than in the non-smokers group. Also, the interburst intervals of the smokers group are longer in median duration than the IBI in the non-smokers group.

Therefore, our preliminary results show that, as physiologically expected, the spontaneous brain activity of a fetus in a nicotine-caused high-risk pregnancy tends to have larger interburst intervals and smaller bursts. In plain words, it seems that when the mother smokes, the spontaneous brain activity is reduced before birth.

We hope this preliminary analysis serves as a contribution for the development of new diagnosis methods based in fetal functional brain activity analysis using completely non-invasive techniques, as well as for providing health guidance aimed at quitting smoking during (and before) pregnancy.

4.4 Limitations of our study

Some of the limitations found were that, since the mothers are asked to perform the study every two weeks, there is little information for some gestational ages. Also, the amount of nicotine in the body of the mother (blood, urine, placenta, hair, etcetera) at the time of the study is not measured, and it can vary from mother to mother. Likewise, since we do not measure the amount of nicotine in the mothers, we are trusting in their word

when they affirm they smoke or do *not* smoke. Furthermore, the burst identification is visual and, as it is done manually, the process is long and prone to subjective interpretation. Besides, we only used one subject for every GA either because of the lack of subjects for specific GAs or due to lack of good datasets (in cases when the head coil was not working, we were not able to use the frequency subtraction method).

Chapter 5

5. Conclusions and future work

5.1 Conclusions

This study adds to the beleif that smoking during pregnancy provokes the fetus to have greater intervals of time without sudden manifestation of brain activity, which can be related to retardation in the brain's maturity.

In a low-risk pregnancy, as the fetus approaches birth, the maturation of the fetal brain accelerates. This can be seen in the diminishing of the interburst intervals' duration and the greater burst's duration.

In smoking mothers, as the fetus approaches birth, the maturation of the fetal brain is slower, as seen in the increase of the duration of interburst intervals and the reduced burst duration.

5.2 Academic internship

This work was developed at the University of Arkansas for Medical Sciences at Little Rock, Arkansas (uams.edu), under the supervision and guidance of Dr. Hari Eswaran, director of SARA Research Center of the Obstetrics and Gynecology Department, and Dr. Diana Irazú Escalona-Vargas, researcher of the same center, from July 1st to December 29th, 2016.

5.3 Future work

Future work will use the acquired brain data to compute the brain rhythms, and identify their behavioral states in order to make a more complete comparison among them. Also, the actogram of every subject can be analyzed to assess the fetal state and compute its correlation with burst and IBI durations (Haddad, et al., 2011).

Bibliography

Anblaan, D., Jones, N. W., Costigan, C., Parker, A. J., Allcock, K., Aleong, R., . . . Gowland, P. A. (2013). Maternal Smoking during Pregnancy and Fetal Organ Growth: A Magnetic Resonance Imaging Study. *PLoS ONE*.

Cartney, J. M., Fried, P., & Watkinson, B. (1994). Central auditory processing in school-age children prenatally exposed to cigaratte smoke. *Neurotoxicol Teratol*, 269-276.

CDC. (2016, October). *ends-key-facts-oct-2016.pdf.* Retrieved from CDC: https://www.cdc.gov/tobacco/stateandcommunity/pdfs/ends-key-facts-oct-2016.pdf

Chi-Yuan, L., Yu-Jung, C., Jia-Fu, L., Chao-Lin, L., & Chia-Hsiang, C. (2012). Cigarettes and the developing brain: Picturing nicotine as a neuroteratogen using clinical and preclinical studies. *Tzu Chi Medical Journal*, 157-161.

Ekblad, M., Korkeila, J., Parkkola, R., Lapinleimu, H., Haataja, L., Lehtonen, L., & PIPARI Study Group. (2015, Jan). Smoking during pregnancy affects foetal brain development. *ActaPaediatr, 104*(1), 12-18.

Escalona-Vargas, D., Siegel, E. R., Murphy, P., Lowery, C. L., & Eswaran, H. (2017). Selection of Reference Channels Based on Mutual Information for Frequency-Dependent Subtraction Method Applied to Fetal Biomagnetic Signals. *IEEE Transactions on Biomedical Engineering, 64*(5), 1115-1122.

Eswaran, H., Govindan, R. B., haddad, N. I., Siegel, E. R., Preissl, H., Murphy, P., & Lowery, C. L. (2012). Spectral Power Differences in the Brain Activity of Growth-Restricted and Normal Fetuses. *Early Human Dev.*, 451-454.

(2017). Fundamentals of the Nervous System. In S. G. Waxman, *Clinical Neruoanatomy, 28e.* New York, New York: McGraw-Hill Education.

Haddad, N., Govindan, R. B., Vairavan, S., Siegel, E., Temple, J. P., Lowery, C. L., & Eswaran, H. (2011). Correlation between fetal brain activity patterns and behavioral states: An exploratory fetal magnetoencephalography study. *Experimental Neurology*, 200-205.

Haynes, W. (2013). Wilcoxon Rank Sum Test. In Dubitzky, Werner, Wolkenhauer, Olaf, Cho, Kwang-Hyun, . . . Hiroki, *Encyclopedia of Systems Biology* (pp. 2354-2355). New York, NY: Springer New York.

Hellstrom-Lindahl, E., & Nordberg, A. (2002). Smoking during pregnancy: a way to transfer the addiction to the next generation? *Respiration*, 289-293.

Kelly, J., Mathews, K. A., & O'Conor, M. (1984). Smoking in pregnancy: effects on mother and fetus. *Br J Obstet Gynaecol*, 111-117.

Lowery, C. L., Govindan, R. B., Preissl, H., Murphy, P., & Eswaran, H. (2009). Fetal Neurological Assessment Using Noninvasive Magnetoencephalography. *Clin Perinatol*, 701-709.

Maestú, C., Gómez-Utrero, E., Piñeiro, R., & Sola, R. (1999). Magnetoencefalografía: una nueva técnica de diagnóstico funcional en neurociencia. *Revista de Neurología*, 1077-1090.

McDonald, J. H. (2014). *Handbook of Biological Statistics.* Retrieved 10 27, 2017, from http://www.biostathandbook.com/wilcoxonsignedrank.html

McDonald, J. H. (n.d.). *Handbook of Biological Statistics*. (Sparky House Publishing) Retrieved 10 27, 2017, from http://www.biostathandbook.com/kruskalwallis.html

Muennsinger, J., Eswaran, H., & Preissl, H. (2014). *Fetal Magnetoencephalography (fMEG).* Springer.

Oliff, H., & Gallardo, K. (1999). The effect of nicotine on developing brain catecholamine systems. *Front Biosci*, 883-897.

Preissl, H., & Lowery, C. L. (2004). Developmental neurosciences: imaging the invisible? *Experimental Neurology*, S1.

Preissl, H., Lowery, C. L., & Eswaran, H. (2004). Fetal magnetoencephalography: current progress and trends. *Experimental Neurology*, S28 - S36.

Preissl, H., Lowery, C. L., & Eswaran, H. (2005). Fetal Magnetoencephalography: Viewing the Developing Brain in Utero. In H. Preissl, *Magnetoencephalography.* Elsevier, Inc.

Regan, A. K., Promoff, G., Dube, S. R., & Arrazola, R. (2013). Electronic nicotine delivery systems: adult use and awareness of the 'e-cigarette' in the USA. *Tobacco Control*(22), 19-23.

Ropper, A. H., Samuels, M. A., & Klein, J. P. (2014). Chapter 28. Normal Development and Deviations in Development of the Nervous System. In *Adams and Victor's Principles of Neurology, 10e.* New York: The McGraw-Hill Companies.

Sheridan, C. J., Matuz, T., Draganova, R., Eswaran, H., & Preissl, H. (2010). Fetal Magnetoencephalography - Achievements and Challenges in the Study of Prenatal and Early Postnatal Brain Responses: A Review. *Infant Child Dev.*, 80-93.

The MathWorks Inc. (n.d.). *Wilcoxon rank sum test*. Retrieved from https://www.mathworks.com/help/stats/ranksum.html

The MathWorks, Inc. (1993-2006). function [p,anovatab,stats] = kruskalwallis(varargin).

Vrba, J., & Robinson, S. E. (2001). Signal Processing in Magnetoencephalography. *Methods*, 249-271.

Vrba, J., McCubbin, J., Govindan, R., Vairavan, S., Murphy, P., Preissl, H., . . . Eswaran, H. (2012). Removal of interference from fetal MEG by frequency dependent subtraction. *NeuroImage, 59*(3), 2475-2484.

Wakai, R. T. (2004). Assessment of fetal neurodevelopment via fetal magnetocardiography. *Experimental Neurology*, S65-S71.